Self Tuning of Cascade PI Controller for Buck Converter Based on Adaptive Interaction

Sabat Anwari

Electrotechnic Departmen of ITENAS Bandung
sabat.anwari @ gmail.com

Abstract

DC–DC converter convert DC voltage signal from high level to low level signal or it can be vise versa depending on the type of converter used in system. Buck converter is one of the most important components of circuit, it converts voltage signal from high DC signal to low voltage. In buck converter, a high speed switching devices are placed and the better efficiency of power conversion with the steady state can be achieved. Its nonlinearities and uncertainties have increased the complexity of associated controllers so desired performance is achieved. However, cascade-PI controllers are still used to address this problem due to its relative implementation easiness, negating the complexity to the tuning strategy. The relative simplicity of system-specific PI control tuning methods enable a desired system response characteristic: robust, rapid error attenuation with minimal overshoot, zero steady-state off-set, to be easily attained. In this paper, an adaptive interaction is adopted to tune PI controller. The method is simple and effective way to perform gradient descent in the parameter space. The tuning algorithm requires no knowledge of the plant to be controlled. This makes the algorithm robust to changes in the plant.

Keywords : buck converter, cascade, PI controller, self tuning, adaptive interaction.

1. Introduction

DC-DC converters with computerized digital control methods picked up ubiquity because of their high productivity, low power utilization, higher resistance to natural changes, for example, temperature and maturing of parts, capacity to interface effortlessly, of programmability and to actualize advanced control plans. Their requisitions incorporate compact electronic gadgets, for example, computer and smart phones others (Mondal, 2014).

A buck converter is a time varying system as its dynamical behavior depends on a switch controlled through PWM; moreover, the relation between the PWM duty cycle and the output voltage is nonlinear (Ibarra, et.al., 2015).

Besides DC/DC converters have been successfully controlled in the past, it was until 90s when its nonlinear characteristics where formally discussed and some advanced control techniques were used to improve their performance. The control objectives have been met before the system was thoroughly understood as stated in (Tse and Bernardo, 2002). However, the convenience of modeling them in a simplified manner has made researchers also to follow this path despite of the need of two different models dependent on current conditions: continuous and discontinuous conduction modes (CCM and DCM). One of the most used methods to achieve linear representation of voltage converters is the Small-signal state-space averaging (Tse and Bernardo, 2002).

Although simpler linear models allow the designer to consider well-known frequency-domain constraints and design techniques, its validity is restricted to a determined bandwidth and can not attain nonlinear behavior; as the linear model is desired to be kept simple, the control loop complexity must be increased through a more dependable controller (Gupta, et.al., 1997). This has lead to an increasing number of works related to control implementation under parametric variations, uncertain environments, and ambiguous measurements which commonly adopts one single control technique and a determined set of tests to validate converter's performance.

The most commonly used control schemes are voltage mode control and current mode control (Dixon, 1985). The former takes the output voltage as its only feedback signal; however, its performance degrades on DCM. The current mode control effectively alleviates the sensitivity of the converter dynamics and could offer near uniform loop gain characteristics for both CCM and DCM operation. The key feature of current

mode control is that the inner loop changes the inductor into a voltage-dependent current source at frequencies lower than crossover frequency of the current loop.

A commonly used way to implement a current mode control is using two Proportional Integral (PI) controllers; one for the inner current loop and one more for the outer voltage one. Furthermore, to improve the robustness, an on-line self tuning PI controller by using adaptive interaction, is proposed. An adaptive interaction technique is used to tune the parameters of PI controller. Our approach is based on a recently developed theory of adaptive interaction (Lin, et. al., 2000). Using this theory, the controlled system is decomposed into three subsystems consisting the plant, the proportional, and the integral. The parameters of PI controller, K_p and K_i are viewed as the interactions between these three subsystems. A general adaptation algorithm developed in the theory of adaptive interaction is applied to self-tuning these coefficients. The algorithm is simple and effective.

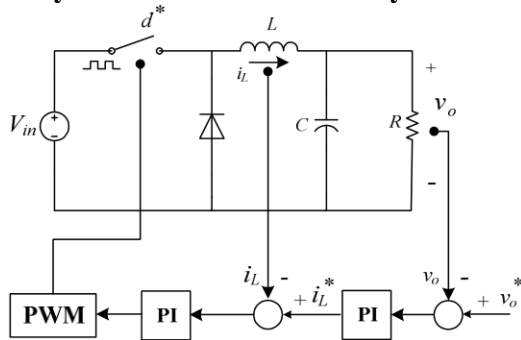## 2. Dynamic Model of Studied System

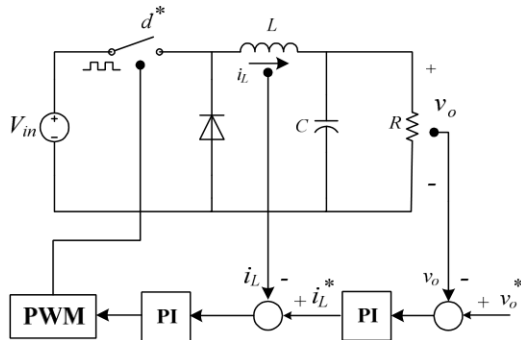Figure 1. The regulated buck converter with a resistive load

Figure 2. The schematic of buck converter controllers

The buck converter considered in this paper is shown in Fig. 1. It consists of a DC voltage source V_{in}, the elements of buck converter represented by L and C, the resistive load R, and the PI controllers of current loop (inner loop) and voltage loop (outer loop) represented by K_{pv}, K_{iv}, K_{pi}, and K_{ii}, respectively.

The schematic of cascade PI controllers for a buck converter is depicted in Fig. 2 (adopted from Chonsatidjamroen, et. al., 2012).

The dynamic model of a controlled buck converter as shown in Fig. 1 derived from the generalized state-space averaging (GSSA) modeling method can be written as:

$$\dot{x} = Ax + B$$
$$y = Cx + Du \tag{1}$$

where state-variable $x = [i_L \quad v_o \quad x_v \quad x_i]^T$, input $u = [v_o^*]$, and output $y = [v_o]$.

The details of A, B, C, D are as follows:

$$A = \begin{bmatrix} -\dfrac{K_{pi}V_{in}}{L} & -\dfrac{K_{pv}K_{pi}V_{in}+1}{L} & \dfrac{K_{iv}K_{pi}V_{in}}{L} & \dfrac{K_{ii}V_{in}}{L} \\ \dfrac{1}{C} & -\dfrac{1}{RC} & 0 & 0 \\ 0 & -1 & 0 & 0 \\ -1 & -K_{pv} & K_{iv} & 0 \end{bmatrix},$$

$$B = \begin{bmatrix} \dfrac{K_{pv}K_{pi}V_{in}}{L} \\ 0 \\ 1 \\ K_{pv} \end{bmatrix}, C = [0 \quad 1 \quad 0 \quad 0], D = [0] \tag{2}$$
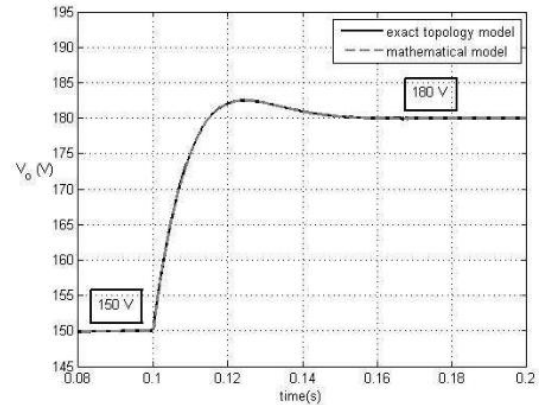

Figure 3. Response of v_o for changing the v_o^* from 150 V to 180 V
(Chonsatidjamroen, et. al., 2012)

The set of parameters for the system in Fig.1 is given as follows: $R = 120\,\Omega$, $R = 15$ mH ($\Delta I = 0.1$ A), $C = 150\,\mu F$ ($\Delta V = 10$ mV), $V_{in} = 200$ V, and $T_s = 0.1$ ms. Fig. 3 shows the comparison of the output voltage responses of the system in Fig. 1 between the exact topology model and the averaging model as given in (1) to a step change of the voltage command v_o^* from 150 V to 180 V that occurs at $t = 0.1$ s. The parameters of PI controllers for Fig. 3 are designed via the classical method by setting the bandwidth of current loop is faster than the bandwidth of voltage loop by 20 times. The PI controller parameters for this case are $K_{pv} = 0.0205$, $K_{iv} = 2.16$, $K_{pi} = 0.2880$, and $K_{ii} = 432$ in which ω_{nv}, ξ_v, ω_{ni}, and ξ_i are equal to 120 rad/s, 0.8, 20*120 rad/s, and 0.8,

respectively. The details how to design the PI controllers using the classical method for buck converter having the schematic as depicted in Fig. 2 can be found in (Tsang and Chan, 2005).

3. Theory of Adaptive Interaction

The theory of adaptive interaction considers a complex system consisting of $\mathcal{N}$ subsystems which we called devices. Each device (indexed by $n \in \mathcal{N} := \{1, 2, \cdots, \mathcal{N}\}$) has an integrable output signal y_n and an integrable input signal x_n. The dynamics of each device is described by a causal functional

$$\mathcal{F}_n : x_n \rightarrow y_n, n \in \mathcal{N} \qquad (5)$$

where x_n and y_n are the input and output spaces repectively. That is, the output $y_n(t)$ of the nth device relates to its input $x_n(t)$ by

$$y_n(t) = (\mathcal{F}_n \circ x_n)(t) = \mathcal{F}_n[x_n(t)], \qquad (6)$$
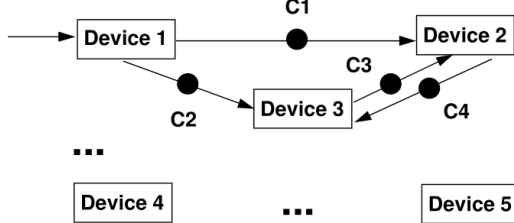
where $\circ$ denote composition.

Figure 4. A typical decomposition of a system for adaptive interaction

We assume the Frechet derivative of $\mathcal{F}_n$ exixts. We further assume that each device is a single input single output system.

An interaction between two devices consists of a functional dependence of the input of one of the devices on the outputs of the others and is mediated by an information carrying connections denoted by c. The set of all connections is denoted by C.

We assume that there is at most one connection from one device to another. Let pre_c be the device whose output is conveyed by connection c and $post_c$ the device whose input depends on the signal conveyed by connection c. We denote the set of input interactions for the nth device by $I_n = \{c : pre_c = n\}$ and the set of output interactions by $O_n = \{c : post_c = n\}$. A typical system is illustrated in Figure 4. In the figure, for example, the set of input interactions of Device 2 is $I_2 = \{c_1, c_3\}$ and the set of output interactions is $O_2 = \{c_4\}$. Also, c_1 connects Device 1 to Device 2, therefore $pre_{c_1} = 1, post_{c_1} = 2$.

For the purpose of this paper, we consider only linear interactions, that is, we assume that the input to a device is a linear combination of the output of other devices via connections in I_n and possibly an external input signal $u_n(t)$:

$$x_n(t) = u_n(t) + \sum_{c \in I_n} \alpha_c y_{pre_c}(t) \qquad (7)$$

where α_c is the connection weights.

With this linear interaction, the dynamics of the system is described by

$$y_n(t) = \mathcal{F}_n\left[u_n(t) + \sum_{c \in I_n} \alpha_c y_{pre_c}(t)\right] \quad (8)$$

To simplify the notation, in the rest of the paper, we will eliminate when appropriate the explicit reference to time t.

The goal of our adaptation algorithm is to adapt the connection weights α_c so that some performance index $E[y_1, \cdots y_n, u_1, \cdots u_n]$ as a function of the external inputs and outputs will be minimized. The algorithm is given in the following theorem (Lin, et. al., 2000):

Theorem 1: For the system with dynamics given by

$$y_n = \mathcal{F}_n\left[u_n + \sum_{c \in I_n} \alpha_c y_{pre_c}\right] \qquad (9)$$

If connection weights α_c are adapted according to

$$\dot{\alpha}_c = -\gamma \frac{\partial E}{\partial y_{post_c}} \circ$$
$$\mathcal{F}'_{post_c}[x_{post_c}] \circ y_{post_c} \qquad (10)$$

and the above equation has a unique solution, then the performance index will decrease monotonically with time. In fact, the following is always satisfied

$$\dot{\alpha}_c = -\gamma \frac{\partial E}{\partial \alpha_c}, c \in C \qquad (11)$$

where $\gamma > 0$ is some adaptation coefficient.

4. Controller Designs

In this section, the controller designs for the buck converter via the classical and adaptive interaction methods are illustrated.

4.1 Classical Method

The details of PI controller design using the classical method can be found in (Tsang and Chan, 2005). The PI parameters for the classical method in this paper are designed by selecting $\xi_v = 0.8$, $\xi_i = 0.8$, $\omega_{ni} = 20 \times 120$ rad/s, and $\omega_{nv} = 120$ rad/s. Hence, the PI controller parameters designed by the classical method are given by $K_{pv} = 0.0205$, $K_{iv} = 2.16$, $K_{pi} = 0.2880$, and $K_{ii} = 432$.

4.2 Adaptive Interaction Method

Let $e_v = v_o^* - v_o$ denote the voltage error and $e_i = i_L^* - i_L$ denote the current error. For a cascade PI control system, we decompose the system into three devices as shown in Figure 2: Device 1 is the proportional part with transfer function 1; Device 2 is the integral part with transfer function s^{-1}; Device 3 is the plant. In this case, there are four adaptive connections: $\alpha_c = K_{pv}$, K_{iv}, K_{pi}, and K_{ii}. Since for all these

connections, $O_{post_c} = O_3 = 0$, the adaptation algorithm of the previous section reduces to

$$\dot{\alpha}_c = -\gamma \frac{\partial E}{\partial y_{post_c}} \circ$$
$$\mathcal{F}'_{post_c}[x_{post_c}] \circ y_{post_c} \qquad (12)$$

We take our goal as to minimize the error

$$E = e^2 \qquad (13)$$

We then obtain the following Frechet tuning algorithm

$$\dot{K}_P = -2\,\gamma\,e\,\mathcal{F}'_3 \circ e \qquad (14)$$

Similarly, we have

$$\dot{K}_I = -2\,\gamma\,e\,\mathcal{F}'_3 \circ e^{int} \qquad (15)$$

where $e^{int} = \int e\,\mathrm{dt}$.

Note that the self tuning algorithm for P and I all have the same form: It depends on the error e, the Frechet derivative, and the output of device.

To calculate the Frechet derivative, let us consider the functional of the following form

$$\mathcal{F}[x] = \int_0^t f(x(\tau), \tau) d\tau \qquad (16)$$

It can be shown (Luenberger, 1968, page 175) that the Frechet differential of $\mathcal{F}$ is equal to its Gateaux differential which is given by

$$\delta\mathcal{F}[x; h] = \int_0^t f_x(x(\tau), \tau) d\tau \qquad (17)$$

where $f_x = \frac{\partial f}{\partial x}$. Therefore, the Frechet derivative of $\mathcal{F}$ at x is given by

$$\mathcal{F}'[x] \circ h = \int_0^t f_x(x(\tau), \tau) d\tau \qquad (18)$$

For a linear time invariant plant with transfer function $\mathcal{F}$ is given by the convolution

$$\mathcal{F}[x] = \int_0^t x(\tau) g(t - \tau) d\tau \qquad (19)$$

where $g(t)$ is the impulse response. Therefore the Frechet derivative

$$\mathcal{F}'[x] \circ h = \int_0^t g(t - \tau) h(\tau) d\tau \qquad (20)$$

For many practical systems, as shown in (Lin, et. al., 2000) the Frechet derivative can be approximated by

$$\mathcal{F}'[x] \circ h = \beta h \qquad (21)$$

where β is some constant.

Substitute the above approximation into the Frechet tuning algorithm, adopted from (Lin, et. al., 2000), self tuning algorithm is as follows

$$\dot{K}_{pv} = -\gamma\,e_v e_v \qquad (22)$$
$$\dot{K}_{iv} = -\gamma\,e_v e_v^{int} \qquad (23)$$
$$\dot{K}_{pi} = -\gamma\,e_i e_i \qquad (24)$$
$$\dot{K}_{ii} = -\gamma\,e_i e_i^{int} \qquad (25)$$

5. Simulation Results

In order to validate the control strategies as described above, digital simulation was carried out on a buck converter, as shown in Figure 1 having the controllers designed by using the classical method and the Selft Tuning Proportional Integral (STPI) controller. The control simulation results are shown in Figure 5 and Figure 6.
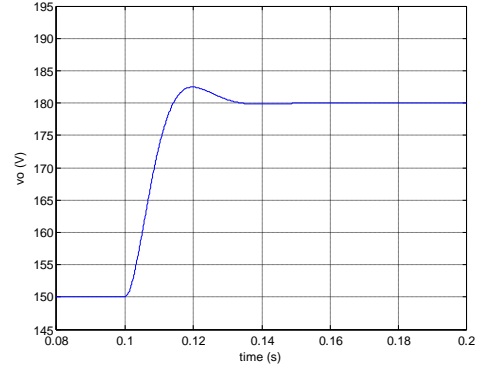

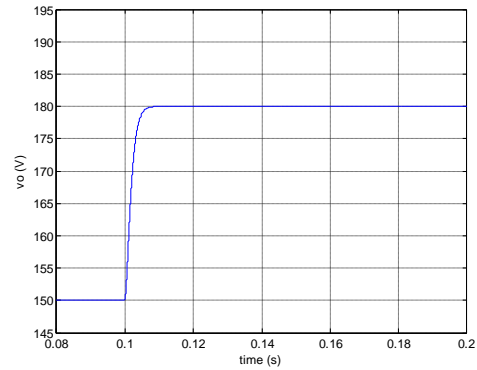*Figure 5. Simulation result of buck converter with a conventional method*

Figure 6. Simulation result of buck converter with a STPI controller

Figure 5 and 6 show the v_o response to a step change of v_o^* from 150 V to 180 V that occurs at $t = 0.1$ second. Figure 5 shows that the response of the buck converter with classical method while Figure 6 depicts the response of the buck converter using Selft Tuning Proportional Integral (STPI) controller. Applying a classical method to the system, the transient response achieved is slightly lower than the STPI. There is no overshoot when STPI is applied while using classical method there is a little overshoot. Results in Fig. 5 and Figure 6 shows that the STPI performs slightly better than the classical method.

6. Conclusions

The control of the buck converter is investigated in this research work with Selft Tuning Proportional Integral (STPI). The conclusion is that STPI is found to be superior, more robust, faster, flexible, and less sensitive to the parameter variations as compared with classical PI controllers. Simulation results are presented to demonstrate the potential of the proposed scheme. It has been shown that the proposed scheme has several advantages such as, small steady state error, fast response, and small overshoot.

References

Chonsatidjamroen, S., Areerak, K. N., Areerak, K. L., and Srikaew, A. (2012) Optimized cascade PI controllers of buck converters using particle swarm optimization algorithm. In *The 11th WSEAS International Conference on Artificial Intelligence, Knowledge Engineering and Data Bases (AIKED'12)*. p. 21-26. Cambridge. United Kingdom, February 22-24.

Dixon, L. (1985) Current-mode control of Switching power supplies. in *Unitrode,* SM400: p. 1–9. United States.

Gupta, T., Boudreaux, R., Nelms, R., and Hung, J. (1997) Implementation of a fuzzy controller for DC-DC converters using an inexpensive 8-b microcontroller. in *IEEE Transactions on Industrial Electronics*, 44 (5). p. 661–669. Oct..

Ibarra, L., Macias, I., Ponce, P., and Molina, A. (2015). On DC/DC voltage buck converter control improvement through the QFT approach. In *New Developments in Circuits, Systems, Signal Processing, Communication and Computers*. p. 183-190.

Lin, F., Brand, R. D., and Saikalis, G. (2000) Self tuning of PID controllers by adaptive interaction. in *Proceedings of the American Control Conference*. Chicago. Illinois, June.

Luenberger, D. G. (1968) *Optimization by Vector Space Methods*. John Wiley & Sons,.

Mondal, A. (2014) Digital PID controller design for DC-DC buck converter. *Master Thesis*. National Institute of Technology. Rourkela. India.

Tsang, K. M. and Chan, W. L. (2005) Cascade controller for DC/DC buck convertor. in *IEE Electric Power Applications*, 152 (4): p. 827-831.

Tse, C. and di Bernardo, M. (2002) Complex behavior in switching power converters. In *Proceedings of the IEEE*, 90 (5): p. 768–781. May.